J Therm Anal Calorim (2010) 99:733–740
DOI 10.1007/s10973-009-0353-4

Adsorption of organic pollutants over microporous solids investigated by microcalorimetry techniques

B. Dragoi · V. Rakic · E. Dumitriu · A. Auroux

MEDICTA2009 Conference

Abstract This work is focused on the gas and liquid-phase adsorption of pollutants: propanol, 2-butanone, phenol and nicotine onto zeolites (H-BETA, H-ZSM-5, H-MCM-22, and clinoptilolite). Textural properties and origin of zeolites were taken into account as criteria of adsorbents selection. The aldehyde and the ketone were adsorbed in the gas phase using microcalorimetry linked to a volumetric line to evaluate adsorption. Adsorptions in water were carried out for phenol and nicotine and the evolved heats during adsorption were measured by a differential heat flow reaction calorimeter with stirring. Results are discussed in relation with the pore sizes and various interactions which could occur between the adsorbent and the adsorbate.

Keywords Adsorption · Depollution · Microcalorimetry · Organic pollutants · Zeolites

Introduction

Volatile organic compounds (VOCs) are among the key pollutants emitted into the atmosphere that cause outdoor air pollution. They are organic compounds that may undergo photochemical reactions yielding even more hazardous compounds. The effects of VOCs on the environment, namely in the depletion of the stratospheric ozone layer, smog formation or direct action on human tissues, are well documented [1]. VOCs emissions originate from transport activities (∼30%), solvent uses (∼20%), industrial processes (∼3%) and various sources (∼47%) [2] and can be placed in different categories, namely (i) chlorinated hydrocarbons (ii) aromatic hydrocarbons (iii) mono- and polyalcohols and (iv) carbonyl compounds [1]. Besides VOCs, alkaloids such as nicotine have an important contribution to the deterioration of water and air quality. The removal of all these pollutants is still a main issue even though various techniques such as thermal, biological and catalytic oxidation, reduction, condensation, refrigeration or adsorption have been developed [3, 4]. Among them, adsorption has been found to be the proper strategy which removes pollutants in an economic way in terms of initial cost, simplicity of design, and ease of operation. Numerous papers on the adsorption of VOCs on activated carbons which possess very high surface area (around 1,000 $m^2\ g^{-1}$) have been already published [5, 6]. However, activated carbons have some disadvantages such as flammability, difficulty to desorb the high-boiling solvents, tendency to promote polymerization or oxidation of some solvents to toxic or insoluble compounds [7]. Due to their porous structure, and high surface areas, zeolites are among the best candidates as adsorbents because they can retain the organic molecules at the surface but also into the pores, the molecular size of the pollutants playing an important role in the last case. Zeolites could be either hydrophilic or hydrophobic having thus, affinity for both polar and non-polar molecules, which favor their use as adsorbents. So far, synthetic (such as BETA, MCM-22, ZSM-5) and

B. Dragoi · E. Dumitriu
Faculty of Chemical Engineering and Environmental Protection, Technical University, 71 A Mangeron Av, 700050 Iasi, Romania

V. Rakic
Faculty of Agriculture, University of Beograd, 11080 Zemun, Nemanjina 6, Serbia

B. Dragoi · A. Auroux (✉)
Institut de Recherches sur la Catalyse et l'Environnement de Lyon, UMR5256 CNRS-Université Lyon 1, 2 av. A. Einstein, 69626 Villeurbanne Cedex, France
e-mail: aline.auroux@ircelyon.univ-lyon1.fr

natural (clinoptilolite) molecular sieves have been used for the adsorption of aliphatic and aromatic hydrocarbons, alkylamine, chlorinated compounds, etc. [8–11].

In the present work, we investigate the adsorption behavior in both gas and liquid phase of three synthetic zeolites (H-BETA, H-MCM-22, H-ZSM-5) and one natural zeolite (clinoptilolite) on three VOCs and one alkaloid (nicotine). VOCs under study belong to different classes of organics such as aldehydes (propanal), ketones (2-butanone) and aromatic compounds (phenol). Carbonyl compounds (propanal and 2-butanone) have been adsorbed in gas phase using microcalorimetry as the key technique to estimate adsorption. Adsorptions of phenol and nicotine have been performed in liquid phase (water) using liquid microcalorimetry as the principal technique.

Experimental

Materials

H-MCM-22 zeolite was hydrothermally synthesized using hexamethylenimine (HMI, $C_7H_{13}N$, 99% purity, Aldrich) as organic template, SiO_2 (Aerosil-200, Degussa), sodium aluminate ($NaAlO_2$ 56% Al_2O_3, 37% Na_2O, Carlo Erba), sodium hydroxide (NaOH 98% purity, Prolabo) and deionized water. The procedure of synthesis is presented in detail in a previous work [12]. *H-ZSM-5* zeolite was supplied by Degussa and *H-BETA* zeolite by Rhône-Poulenc while the natural *clinoptilolite* ($Ca_{3.38}Mg_{0.38}Na_{1.5}K_{1.03}(Al_{6.3}Si_{29.7}O_{72})\cdot 21H_2O$; denoted as Clino) is taken from Zlatokop deposit in Serbia and Montenegro.

Characterization

X-ray diffraction measurements were performed on a Bruker D5005 apparatus between 3° and 80° (2θ) using CuKα radiation ($\lambda = 1.54184$ Å). *The textural properties* were determined by nitrogen adsorption at 77 K after pretreatment for 4.0 h at 673 K under vacuum. ^{29}Si NMR and ^{27}Al NMR spectra have been recorded at 104.27 and 79.5 MHz, respectively, on a Bruker DSX 400 spectrometer.

Gas phase microcalorimetry

The experiments were carried out in a microcalorimeter of Tian–Calvet type (C80 from Setaram) linked to a volumetric line that makes possible to study the gas–solid interactions. For the estimation of the acidic properties, NH_3 and pyridine (denoted as Py) were chosen as basic probe molecules. Adsorption capacities of the samples were checked on the adsorption of two organic groups, namely aldehydes (propanal; denoted as PAL), and ketones (2-butanone or methylethylketone denoted as MEC). Samples were pretreated under vacuum at 623 K overnight. The adsorption experiments consisted in sending repeatedly small doses of gas onto the solid while recording the heat flow signal and the concomitant pressure evolution until an equilibrium pressure of $\sim$67 Pa was reached. The adsorptions were carried out at 303, 353 and 423 K for VOCs, NH_3 and Py, respectively. A readsorption was performed after outgassing the samples for 0.5 h at the same temperatures in order to determine the chemisorbed uptake (V_{irr}).

Titration microcalorimetry

The adsorption heats of aniline (C_6H_7N, 99.5%, Aldrich) diluted in *n*-decane ($C_{10}H_{22}$, 99%, Sigma), phenol (C_6H_6O, 99%, Lancaster) and nicotine ($C_{10}H_{14}N_2$, 99%, Fluka) dissolved in water were measured in a differential heat flow reaction calorimeter equipped with a stirring system (TITRYS, from Setaram). A programmable syringe pump (PH 2000, Harvard Apparatus) was linked to the calorimeter by capillary tubes. Using this syringe pump, successive pulse injections of known amounts of a solution ($\sim$0.03 M) of the probe were sent onto the sample maintained at 308 K at 2 h time intervals. A preheating furnace allowed the injection of the solution at the same temperature as the calorimeter. The reference and measurement cells contained the pure solvent (1.5 mL) and the solvent with a weighted amount of the outgassed solid sample (ca. 150 mg), respectively. The samples were pretreated under vacuum at 623 K for 4 h before being transferred into the calorimeter cell. Each dose was accompanied by an exothermic peak. The evolved heat was evaluated by the SETSOFT acquisition and processing software from SETARAM and represented as a function of the probe amount injected.

Results and discussion

Physico-chemical characterization of samples

The physico-chemical characteristics of samples are listed in Table 1 which gives the Si/Al ratio (from chemical analysis—CA), S_{BET}, pore volumes as well as pore size for each sample.

It is worth to mention that in microporous materials, the adsorbed N_2 molecules fill the pores completely and, because of the limited space, multilayer adsorption is suppressed. Therefore, the BET surface area can only be used as a purely empirical value to compare the quality and porosity of materials of the same kind [13]. Figure 1 shows the XRD patterns containing peaks at values of 2θ which, together with the peak intensities, are characteristic of

Table 1 Textural properties of zeolites

Solid	IZA cod	Si/Al (CA)	S_{BET}/ $m^2\ g^{-1}$	V_{micro}/ $cm^3\ g^{-1}$	V_{total}/ $cm^3\ g^{-1}$	General features	
						Dimensionality	Pore size/nm[a]
Clino		4.7	43	0.009	0.09	2D	{0.31 × 0.75 + 0.36 × 0.46}–0.28 × 0.47
H-ZSM-5	MFI	14.0	392	0.17	0.18	3D	{0.51 × 0.55–0.53 × 0.56}
H-BETA	BEA	12.5	741	0.22	0.68	3D	0.66 × 0.67–0.56 × 0.56
H-MCM-22	MWW	12.5	493	0.18	0.43	2D	0.40 × 0.55|0.41 × 0.51

[a] Atlas of Zeolite Framework Types

zeolites used in this study. The different morphologies of these zeolites are presented in our previous work [12].

Figure 2 illustrates ^{27}Al NMR and ^{29}Si NMR spectra for zeolites. Taking into account the ^{27}Al NMR spectra, the samples can be divided in two groups. The first group includes Clino and H-ZSM-5 whose aluminium atoms are mainly placed in the framework (AlO_4) giving signals at 51.73 and 55 ppm, respectively. However, Clino contains an insignificant part of octahedral aluminium (AlO_6) represented by a small signal at 2.99 ppm. The second group regards H-BETA and H-MCM-22 zeolites. Their ^{27}Al NMR spectra possess two different signals confirming the existence of aluminium in both tetrahedral (54 ppm (H-MCM-22), 55 ppm (H-BETA)) and octahedral (0 ppm (both zeolites)) coordinations.

As Abejado et al. reported [14], the ^{29}Si NMR spectrum for H-BETA zeolite has silicon without any neighboring aluminium atoms (Si(0Al)), which is signaled by the chemical shifts at −115 and −111.6 ppm. A shoulder at −107.5 ppm is attributed to silicon atom placed near an aluminium atom (Si(1Al)). Also, ^{29}Si NMR spectrum of H-ZSM-5 indicates two silicon species in its framework. The first one concerns silicon (Si(0Al)), which gives a signal at −111.5 ppm while the second one is a Si(1Al) type with a chemical shift at −105.8 ppm. H-MCM-22 has a ^{29}Si NMR spectrum including an ensemble of peaks whose chemical shifts are as follows: −119.23; −115.43; −113.53; −111.14; −104.81; −100.02 ppm. All these values confirm the presence of various types of silicon in the H-MCM-22 framework. ^{29}Si NMR spectrum of Clino shows many chemical shifts such as −110.76; 104.76; 98.67; 92.08 ppm, which are typical of (Si(0)Al, Si(1)Al, Si(2)Al, Si(3)Al atoms.

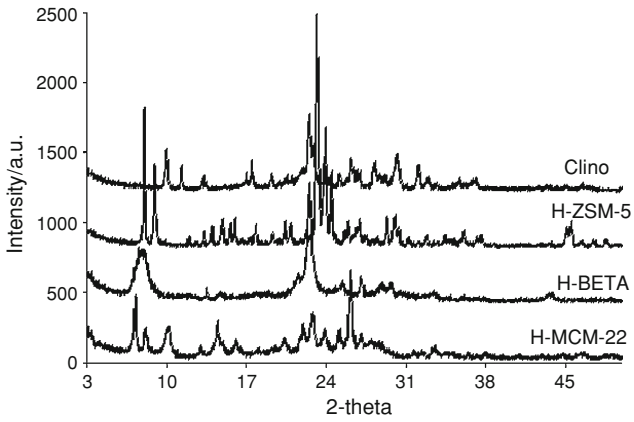

Fig. 1 X-Ray diffractograms of zeolites

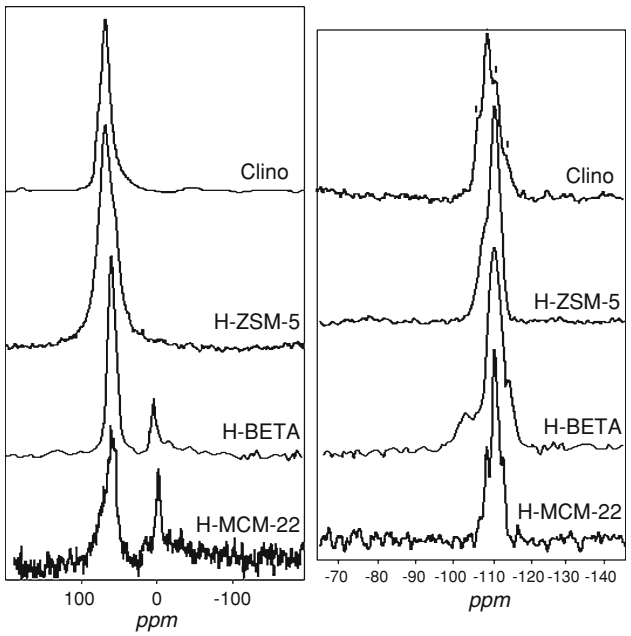

Fig. 2 ^{27}Al NMR spectra of zeolites (*left*) and ^{29}Si NMR (*right*)

Acid properties of samples

To evaluate the acid character of samples gas phase adsorption microcalorimetry was used. Ammonia (pK_a = 9.24, proton affinity = 857.7 kJ mol^{-1}) and Py (pK_a = 5.19, proton affinity = 922.2 kJ mol^{-1}) were chosen to probe the overall acidity of the solids, since both Lewis and Brönsted acid sites retain these molecules. Generally, heat evolved during the adsorption of a molecule on a solid surface at a constant temperature is known as differential heat of adsorption ($Q_{diff} = \partial Q_{int}/\partial n_a$), and it is determined as a function of the surface coverage (n_a). It is claimed that the evolved heat during the adsorption of a basic molecule on an

Table 2 Acid properties of samples

Solid	Total number of acid sites/μmol g^{-1}		Number of strong acid sites/μmol g^{-1}		Integral heat/J g^{-1}		Average heat/kJ mol^{-1}	
	NH_3	Py	NH_3	Py	NH_3	Py	NH_3	Py
Clino	1,609	208	852	128	157	7	95	34
H-ZSM-5	1,137	780	720	668	134	151	118	188
H-BETA	720	932	438	660	81	130	112	135
H-MCM-22	855	795	495	462	97	110	115	131

acid site, reflects the strength of this site. Moreover, the dependence of the heat of adsorption on coverage provides information about heterogeneity of the acid strength [15]. Table 2 summarizes the acidity measurement results obtained from NH_3 adsorption at 353 K and Py adsorption at 423 K, respectively, by giving the total number of acid sites (in μmol probe per gram of sample) at the equilibrium pressure of 27 Pa, the number of strong acid sites (derived from the irreversibly adsorbed probe volume), the integral heat at 27 Pa (in J g^{-1}), the average differential heat (integral heat divided by probe uptake) over the 0–27 Pa range. Following order of acidity (both in number and strength of acid sites) can be given: Clino > H-ZSM-5 > H-MCM-22 > H-BETA. Detailed discussion on the acidity of the studied zeolites is provided in our previous work [12].

The acidity studies in gas phase were fulfilled with a study in liquid phase. Contrary to gas phase, in liquid media the adsorption is accompanied by complex phenomena. In this case, the active sites are covered by liquid which first of all has to be removed before the probe molecules are retained by the solid. Depending on the strength of the acid sites, some of them could react with the solvent, thus preventing activity of these sites towards the probe. On the other hand, the solvent nature has a great influence on the strength of the acidic or adsorption sites of the solid [16]. The molecular interactions which can take place in the liquid phase are as follows: solvent–solid, solvent–solvent, solvent–probe molecule, solid–probe molecule, and probe molecule–probe molecule. These complex relationships have influence on the acidity of a solid in liquid phase. Knowledge of the behavior of the solid in liquid media provides key information for finding the most appropriate solid–solvent–probe molecule triad when the maximum performance of the solid either as catalyst or adsorbent is desired. Moreover, the combination of adsorption gas phase microcalorimetry with titration microcalorimetry gives more complete and realistic information about the overall acidity of the solid.

The surface of zeolites was titrated by aniline solved in n-decane. The evolved heat for each injected dose was recorded as a function of time. The surfaces corresponding to each heat peak decreases as the amount of doses increases. The first probe molecules adsorb easier on the active sites and the evolved heat is higher. Figure 3 illustrates the evolved heats for each dose (calculated from peaks areas) as a function of the amount of aniline sent on zeolites. It can be noticed that the evolved heat for the first doses is between 8 and 4 J g^{-1}. Taking into account these values, the most acidic is H-MCM-22 followed by H-ZSM-5, H-BETA, and Clino. Moreover, it is pointed out that in liquid phase, the acidity scale of the studied zeolites is not preserved in relation to that obtained in the gas phase. The next doses will find a partial occupied surface by probe molecule and, consequently, a lower number of molecules will be adsorbed that will decrease the amount of evolved heat. As a result, the last values of the evolved heats are between 1.2 and 0.18 J g^{-1}.

How this changed order of the acidity could be explained? First of all, it could be supposed that, due to the competition between solvent and probe, in liquid phase the active sites are not occupied depending on their acid strength but rather depending on their ability to liberate the solvent. The evolved heats measured upon aniline adsorption are in fact the sums of the contributions of two effects: the exothermic enthalpy of neutralization of the acid site, ΔH_{neut} and the endothermic enthalpy of the solvent displacement, ΔH_{dpl}, respectively. Regarding the thermal effects due to other phenomena such as stirring, dispersion, dilution and solvation by decane, these are compensated by the reference cell, which contains the solvent only [16, 17]. Structural organization of particular framework of the

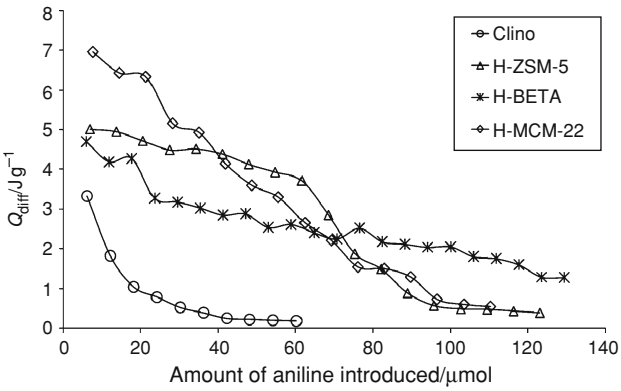

Fig. 3 Evolved heat for each dose of aniline as a function of the amount of probe sent onto the samples in *n*-decane

zeolites studied herein could be considered as additional enlightenment, as well. Due to its size, the decane could occupy the tight channels of zeolites and thus, some active sites are not able to be accessible to the probe. On the other side, H-MCM-22 possesses supercages of 12MR where the solvent could be easier replaced by the probe and therefore, a higher number of active sites are exposed to the probe.

Adsorptive properties of samples in liquid phase

Figure 4 illustrates the differential heats as a function of the amount of nicotine sent onto the samples. The evolved heats for the first doses have values between 2.3 and 0.5 J g^{-1} which give the following order of the samples capacity to retain adsorbate: H-ZSM-5, H-BETA, H-MCM-22, and Clino. The same trend is noticed for the second dose, as well. Starting with the third dose, a completely different behavior is observed for H-BETA. The evolved heat keeps being high although the amount of sent nicotine increases. The final evolved heat is around 0.8 J g^{-1}. The other three zeolites exhibit an expected behavior, namely the evolved heats decrease as the amount of sent probe increases. Moreover, starting with almost 40 μmol of nicotine, the evolved heats for nicotine adsorption on H-ZSM-5 and Clino are almost identical and have the same value, around 0.3 J g^{-1}, which is almost 3 times less in comparison to the final heat in the case of nicotine adsorption on H-BETA. The shape of the calorimetric curves could give an idea on both the localization of the adsorption sites in zeolite structures and their strength, as well. H-ZSM-5 seems to have few stronger sites for nicotine adsorption ($Q_{diff} = 2.1$ J g^{-1}). Sharp decrease of the adsorption heat could indicate that these sites are mainly placed inside of channels. Once these sites are covered by the nicotine molecules, adsorption occurs at the solid surface where only lower acid sites are found [18]. Adsorption of nicotine on H-MCM-22 led to lower adsorption heats ($\sim$1.2 J g^{-1}) and the curve profile is almost similar to that obtained for nicotine adsorption on H-ZSM-5. In the case of H-MCM-22, it can be supposed that the evolved heats for the first five doses are a sum of the heats evolved by the nicotine adsorption on the sites placed in both the channels and 12MR cavities. After covering these sites, the adsorption takes place on zeolite surface and the evolved heats are low and almost constant ($\sim$0.3 J g^{-1}). Concerning Clinoptilolite, the low accessibility to the adsorption sites is quite evident. The nicotine is a relatively bulky molecule and because the pores of this zeolite are, on the one side, small and on the other side, they are fulfilled by cations, the heat evolved for nicotine adsorption is low (below 0.7 J g^{-1}) and mainly invariable. It seems that in this case, the adsorption is performed only at its external surface.

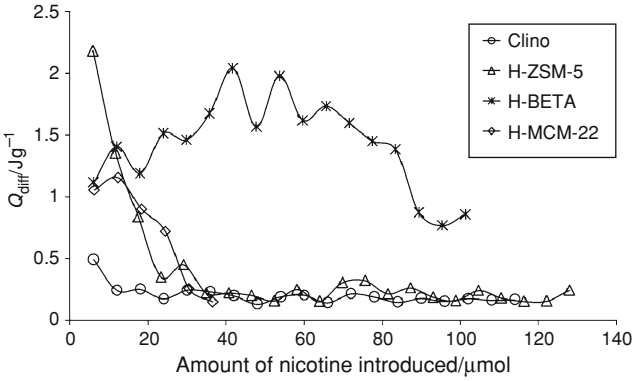

Fig. 4 Evolved heat for each dose of nicotine as a function of the amount of probe sent onto the samples in water

As the adsorption occurs at the solid/solution interface, many factors associated to the nature of solved molecule, solvent and solid properties, respectively, have to be taken into consideration. Concerning the behavior of the nicotine during the adsorption process onto studied porous solids, three factors have to be taken into account such as (i) acid–base interaction of the nicotine with solids, (ii) solvatation phenomenon of the nicotine in aqueous solutions and (iii) the conformations of the nicotine in water knowing that the conformation of the nicotine and its alkalinity in the aqueous phase are different from those in gas phase [19].

The alkaloids like nicotine are considered organic amines (R–NH_2) [20], and thus they are able to be trapped by acid solids *via* a neutralization mechanism supposing that the solid possesses Brönsted acid sites:

$$\text{Solid}-\text{H} + \text{R}-\text{NH}_2 \leftrightarrow [\text{Solid}^-][\text{NH}_3^+-\text{R}] \quad (1)$$

In aqueous solution, the nicotine could be found in three different forms such as neutral, monocation and bication, respectively. At pH equal to 9 (the pH of the 0.03 M solution), the concentrations of monocation and bication species are insignificant, therefore the nicotine is mainly in its neutral form. The nicotine mol ecule possesses two acceptor sites, i.e., the nitrogen atoms of the pyridine ring and pyrrolidine ring, respectively. But which is the most basic? There are many studies which intend to answer to this question [21, 22]. The existence of the two nitrogen atoms in the nicotine molecule implies two pK_a values: 3.10 and 8.01, respectively, at 298 K in water. On the other hand, if the model molecules *N*-methyl-pyrrolidine and pyridine are taken into account, it could be observed that the *N*-methyl-pyrrolidine (pK_a = 10.46) is a stronger Brönsted base than pyridine (pK_a = 5.2). When the basicity of nicotine is evaluated from the side of *N*-methyl-pyrrolidine, the basicity of pyrrolidine nitrogen is decreased by the electron withdrawing effect of the 2-(3-pyridyl) substituent. When the basicity is evaluated from the side of pyridine, the basicity is slightly increased by the weak

electron donating effect of the 3-(*N*-methylpyrrolidin-2-yl) substituent. So, it is considered that in water, the first protonation of nicotine molecule, with $pK_a = 8.01$, takes place on the nitrogen of *N*-methyl-pyrrolidine ring [21]. On the other side, the Brönsted groups are dissociated in diluted aqueous solutions. When the nicotine makes contact to the zeolite suspension, it is preferentially protonated at sp^3 nitrogen. De Lucas et al. [20] performed experiments of nicotine adsorption on acid ion exchange resins. They proposed five equilibrium equations corresponding to those five possible interactions between nicotine and active sites of the resin. The first two possibilities refer to the bication (N^{2+}) and monocation (N^+) forms of the nicotine as follows:

$$N^{2+} + 2R - H \leftrightarrow R_2 - N + 2H^+ \quad (2)$$

$$N^+ + R{-}H \leftrightarrow R{-}N + H^+ \quad (3)$$

At pH = 9, when the nicotine is mainly as neutral form, it could bind on the acid solid *via* one nitrogen or both as it is represented below:

$$N + R{-}H \leftrightarrow R{-}N \quad (4)$$

$$N + 2R{-}H \leftrightarrow R_2{-}N \quad (5)$$

The last possibility relates to the monocation (N^+) that could be adsorbed by two sites:

$$N^+ + 2R{-}H \leftrightarrow R_2{-}N + H^+ \quad (6)$$

Adapting this model to our systems and keeping in mind that the pH of the work solution is 9, it can be pointed out that the nicotine adsorption over zeolites takes place *via* an acid–base reaction according to Eqs. 1, 4 and 5.

Regarding the nicotine conformation in the aqueous solution, Graton et al. [19] have found the following situations. When a water molecule forms a hydrogen bond with either of those two nitrogen atoms, the nicotine conformation does not change itself. Slight change is observed when a water molecule is concomitantly bonded to both nitrogen atoms of the nicotine. Nevertheless, when a second water molecule is bonded to the stable nicotine–water complex, it will induce an important distortion of the nicotine molecule. This distortion allows these water molecules to make a bridge between the two nicotine rings. In these conditions, the conformation of the nicotine is modified by a rotation of 33° between pyridine and pyrrolidine rings, which corresponds to a significant intramolecular disorder. Recently, Elmore et al. [23] have studied the conformations of the nicotine in water and established that *trans* isomer (particularly, *trans* A isomer) is preferred to *cis* isomer.

Figure 5 shows the differential heats of adsorption as a function of the amount of phenol sent on zeolites. Although the phenol adsorption over zeolites is already reported in the literature [24–26], there is no study on the evolved heat during the phenol adsorption in aqueous phase.

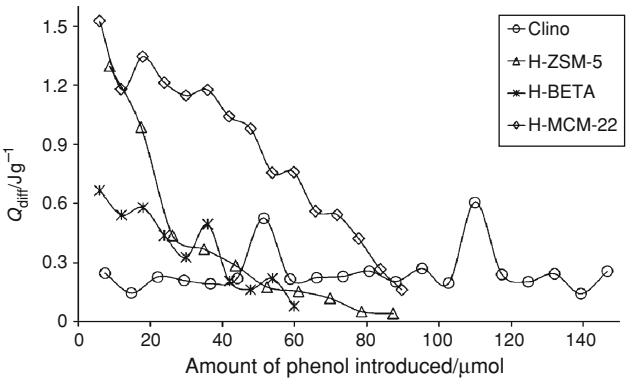

Fig. 5 Evolved heat for each dose of phenol as a function of the amount of probe sent onto the samples in water

The phenol is an acid that exists in aqueous solutions as both neutral and deprotonated forms [25, 27]. The ratio between these two forms is depending on the solution pH. At pH equal to 5 (the pH of the 0.03 M solution), the phenol should be as non-dissociated form [25, 26].

The adsorption heat curves indicate the following order for our zeolites: H-MCM-22 > H-ZSM-5 ≅ H-BETA > Clino. Khalid et al. [24] have performed the phenol adsorption in wastewater on different zeolites. They examined the influence of the Si/Al ratio and the influence of the pores structure, as well. They noticed an improvement of the adsorption capacity when the hydrophobicity of zeolite is increased. The same result has been obtained by Shu [28] when adsorbing phenol and phenol derivates on silicates with Si/Al = 126 and 106, respectively. Our experiments revealed lower evolved heats for phenol adsorption on zeolites in comparison to nicotine adsorption on the same samples. The acidity of phenol prevents the possibility of classical adsorption over the acid sites by a neutralization reaction. Therefore, the forces governing the adsorption are different. However, it is noticed that the evolved heats for phenol adsorption over Clino does not exceed 0.5 J g^{-1} as in the case of nicotine adsorption. Better adsorption of phenol on H-MCM-22 with a heterogeneous distribution of the adsorption sites was noticed, while H-ZSM-5 as well as H-BETA exhibit intermediary adsorption capacity between H-MCM-22 and Clino. Two regions could be delimited in the heat curves obtained for H-ZSM-5 and H-BETA; one corresponding to phenol adsorption onto heterogeneous adsorption sites (until ~40 µmol) and the other one due to the adsorption on weakness and more homogeneous sites (~40–~90 µmol).

In water, the Brönsted sites of zeolite are dissociated according to Brönsted theory. The hydrogen of phenol is attracted by the oxygen atoms of the zeolite framework [29]. The resulting phenolate ion is stabilized by the

existence of many resonance structures. The two *ortho* and *para* positions of the aromatic ring become susceptible to receive a proton or a cation. This is done *via* shifting of π electrons of the aromatic ring. Su et al. [11] have also found that the hydrogen atoms of the aromatic ring are able to interact with oxygen atoms of the zeolite framework. All these interactions strongly depend on zeolite type, Lewis basicity of the framework oxygens and amount of sent phenol. Other factors implied in the phenol adsorption over zeolites are the molecular dimensions of the phenol, the pores size of zeolites and generally, the 3D architecture of the zeolite. Molecular dimensions of phenol are $0.80 \times 0.67 \times 0.15$ nm [6]. Because it is a quite small molecule, it seems that phenol is more suitable to go through the "cups" of 12 MR of the H-MCM-22 which could explain the higher adsorption over this zeolite than on the others. Concerning Clino, it has cations that could adsorb phenol by interactions between these cations and π electrons of the aromatic ring. The main drawback is that these cations are placed into the channels of zeolite, which make difficult the access of phenol. So, the interaction of the aromatic ring with the cations located near the pore inlet could be the only explanation for the adsorption behavior of Clino.

Adsorptive properties of samples in gas phase

The adsorption capacities for the removal of some VOCs such as MEC and PAL from the gas phase have been probed for the samples investigated in this work. Table 3 summarizes the adsorption capacities and corresponding evolved heats for the MEC adsorption over zeolites at 303 K.

The lowest adsorption corresponds to Clino. The integral as well as average heats values show H-ZSM-5 having the stronger adsorption sites while according to the total number of sites, H-MCM-22 adsorbed more MEC than the other three zeolites, closely followed by H-ZSM-5.

PAL adsorption over zeolites was recorded as extremely large heat peaks starting to the equilibrium pressure of 2.7 Pa. This behavior indicates the beginning of a chemical reaction between PAL molecules already adsorbed over zeolites surface. Aldol condensation of the aldehydes takes place in mild conditions and so, PAL adsorption over zeolites at 303 K favors this chemical process. Because the aim of this study was the estimation of the adsorption capacity of these microporous solids, we did not continue to measure the adsorption until a final equilibrium pressure of 67 Pa.

MEC and PAL molecules possess a carbonyl function (C=O). This group contains sp^2 carbon and sp^2 oxygen, respectively. C–O bond has an exposed π electron pair. The oxygen possesses two not-shared electron pairs which confer basic character to the carbonyl group and it can adsorb on the Brönsted and Lewis sites in zeolites. The basicity of this carbonyl group could be affected by the substituent of the carbonyl carbon. The ketone presents a methyl group linked to the carbonyl carbon. This substituent manifests a positive inductive effect ($+I$) that will increase the electronic density around the carbonyl oxygen. This way, the availability of the oxygen electrons pair is increased and this oxygen will be more basic than that existing in PAL molecule.

The adsorption of a carbonyl compound on a Brönsted acid site leads to a carbocation. The adsorption over an aluminium Lewis site is achieved by the electrons pairs of the carbonyl oxygen [30]. In the case of PAL, the resulted carbocation interacts with another aldehyde molecule (as the enol form) leading to an aldol. A water molecule is released and α, β-unsaturated aldehyde is formed. In the case of the ketone, these condensation products could also form but the equilibrium does not favor them. The ketones are less reactive than aldehydes in the nucleophilic additions because of the steric and electronic effects. Consequently, it seems that the ketone remains as adsorbed form without any further chemical reaction. In order to explain how a ketone could interact with the adsorption sites, Jiao et al. [31] have adsorbed acetone on H-Y zeolite and they followed the efficiency of the adsorption by NMR. They found that the carbonyl groups adsorb on the Brönsted sites *via* hydrogen bond while on Lewis sites, the acetone forms complexes. Moreover, they noticed the presence of the aluminium species as pentahedral and octahedral coordinations, respectively, after acetone adsorption. They attributed these species to the coordination of one molecule or two molecules, respectively, on the framework aluminium as in Scheme 1.

Table 3 Adsorptive properties of zeolites based on MEC adsorption at 303 K

Solid	Total number of sites/ μmol g^{-1}	Number of strong sites/ μmol g^{-1}	Integral heat/J g^{-1}	Average heat/ kJ mol^{-1}
Clino	146	67	12	79
H-ZSM-5	1,426	1,042	162	113
H-BETA	1,398	885	131	91
H-MCM-22	1,490	967	141	77

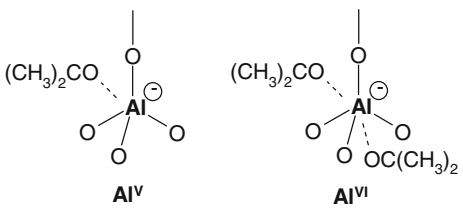

Scheme 1 Coordination species of aluminium with acetone according to Jiao et al. [31]

Conclusions

This paper reports on the behavior of four zeolites (H-BETA, H-ZSM-5, H-MCM-22, and Clinoptilolite) with different channels architectures, pore sizes, surface areas and origins (three synthetic zeolites and one natural zeolite) in the adsorption of three VOCs (PAL, MEC, and phenol) and one alkaloid (nicotine), respectively. Physico-chemical characterization of the samples underlined the high quality of zeolites in the current work. Nicotine adsorption over zeolites led to higher adsorption heats (up to 2.1 J g^{-1} for H-ZSM-5) in comparison to phenol adsorption for which the evolved heat did not exceed 1.5 J g^{-1} (for H-MCM-22). In both cases (nicotine and phenol adsorption, respectively) the lowest evolved heats (below 0.5 J g^{-1}) have been recorded for Clino indicating this solid as not suitable for the removal from the wastewaters of VOCs under study. Among zeolites considered herein, H-ZSM-5 contains the strongest adsorption sites for MEC while H-MCM-22 is able to trap the highest amount of this molecule. For PAL, the adsorption over zeolites as a depollution procedure is not proper due to the occurrence of a chemical reaction already in the first steps of the adsorption.

References

1. Pires J, Carvalho A, de Carvalho MB. Adsorption of volatile organic compounds in Y zeolites and pillared clays. Microporous Mesoporous Mater. 2001;43:277–87.
2. Guisnet M, Gilson JP, editors. Zeolites for cleaner technologies. London: Imperial College Press; 2002.
3. Lewandowski DA. Design of thermal oxidation systems for volatile organic compounds. Florida: CRC Press; 1999.
4. U.S. Environmental Protection Agency: www.epa.org.
5. Basso MC, Cukierman AL. *Arundo donax*-based activated carbons for aqueous-phase adsorption of volatile organic compounds. Ind Eng Chem Res. 2005;44:2091–100.
6. Tanthapanichakoon W, Ariyadejwanich P, Japthong P, Nakagawa K, Mukai SR, Tamon H. Adsorption–desorption characteristics of phenol and reactive dyes from aqueous solution on mesoporous activated carbon prepared from waste tires. Water Res. 2005;39:1347–53.
7. Tsai WT. A review of environmental hazards and adsorption recovery of cleaning solvent hydrochlorofluorocarbons (HCFCs). J Loss Prev Process Ind. 2002;15:147–57.
8. Long YC, Jiang HW, Zeng H. Sorbate/framework and sorbate/sorbate interaction of organics on siliceous MFI type zeolite. Langmuir. 1997;13:4094–101.
9. Corma A, Corell C, Pitrez-Pariente J, Guil JM, Guil-Lopez R, Nicolopoulos S, et al. Adsorption and catalytic properties of MCM-22: the influence of zeolite structure. Zeolites. 1996;16:7–14.
10. Pilchowski K, Chmielewská E. Adsorptive separation of 1,2-dichloroethane from model wastewater by natural clinoptilolite. Acta Hydrochim Hydrobiol. 2003;31:249–52.
11. Su BL, Norberg V, Hansenne C, de Mallmann A. Toward a better understanding on the adsorption behavior of aromatics in 12R window zeolites. Adsorption. 2001;6:61–71.
12. Dragoi B, Gervasini A, Dumitriu E, Auroux A. Calorimetric determination of the acidic character of amorphous and crystalline aluminosilicates. Thermochim Acta. 2004;420:127–34.
13. Jentis A, Lercher JA. Techniques of zeolite characterization. In: Van Bekkum H, Flamingen EM, Jacobs PA, Jansen JC, editors. Introduction to Zeolite Science and Practice, Elsevier, Stud Surf Sci Catal 2001;**137**: 345–386.
14. Adebajo MO, Long MA, Frost RL. Spectroscopic and XRD characterisation of zeolite catalysts active for the oxidative methylation of benzene with methane. Spectrochim Acta A. 2004;60:791–9.
15. Auroux A. Acidity and Basicity: Determination by Adsorption Microcalorimetry, Molecular Sieves, vol. 6. Berlin: Springer; 2008. p. 45–152.
16. Carniti P, Gervasini A, Bennici S. Experimental and modelization approach in the study of acid-site energy distribution by base desorption. Part I: modified silica surfaces. J Phys Chem B. 2005;109:1528–36.
17. Koujout S, Brown DR. The influence of solvent on the acidity and activity of supported sulfonic acid catalysts. Catal Lett. 2005;98:195–202.
18. de Macedo JL, Dias SCL, Dias JA. Multiple adsorption process description of zeolite mordenite acidity. Microporous Mesoporous Mater. 2004;72:119–25.
19. Graton J, van Mourik T, Price SL. Interference between the hydrogen bonds to the two rings of nicotine. J Am Chem Soc. 2003;125:5988–97.
20. de Lucas A, Canizares P, Garcia MA, Gomez J, Rodriguez JF. Recovery of nicotine from aqueous extracts of tobacco wastes by an H^+-form strong-acid ion exchanger. Ind Eng Chem Res. 1998;37:4783–91.
21. Graton J, Berthelot M, Gal JF, Girard S, Laurence C, Lebreton J, et al. Site of protonation of nicotine and nornicotine in the gas phase: pyridine or pyrrolidine nitrogen? J Am Chem Soc. 2002;124:10552–62.
22. Casanova H, Araque P, Ortiz C. Nicotine carboxylate insecticide emulsions: effect of the fatty acid chain length. J Agric Food Chem. 2005;53:9949–53.
23. Elmore DE, Dougherty DA. A computational study of nicotine conformations in the gas phase and in water. J Org Chem. 2000;65:742–7.
24. Khalid M, Joly G, Renaud A, Magnoux P. Removal of phenol from water by adsorption using zeolites. Ind Eng Chem Res. 2004;43:5275–80.
25. Li Z, Burt T, Bowman RS. Sorption of ionizable organic solutes by surfactant-modified zeolite. Environ Sci Technol. 2000;34:3756–60.
26. Hashizume H. Adsorption of some aromatic compounds by a synthetic mesoporous silicate. Environ J Sci Health A Toxic/Hazard Subst Environ Eng. 2004;39:2615–25.
27. Fessenden RJ, Fessenden JS. Organic chemistry. 5th ed. Pacific Grove, California: Brooks/Cole Publishing Company; 1994.
28. Shu HT, Li D, Scala AA, Ma YH. Adsorption of small organic pollutants from aqueous streams by aluminosilicate-based microporous materials. Sep Purif Technol. 1997;11:27–36.
29. Beutel T, Su BL. Behavior of phenol (phenol-d_5) on NaX zeolite as studied by ^{1}H NMR and FT-IR techniques. Chem Phys Lett. 2005;416:51–5.
30. Dumitriu E, Hulea V, Fechete I, Auroux A, Lacaze J, Guimon C. The aldol condensation of lower aldehydes over MFI zeolites with different acidic properties. Microporous Mesoporous Mater. 2001;43:341–59.
31. Jiao J, Kanellopoulos J, Behera B, Jiang Y, Huang J, Marthala RVR, et al. Effects of adsorbate molecules on the quadrupolar interaction of framework aluminum atoms in dehydrated zeolite H,Na-Y. J Phys Chem B. 2006;110:13812–8.